

Electron-Catalyzed Mutual Neutralization of Various Anions with Ar^+ : Evidence of a New Plasma Process

Nicholas S. Shuman, Thomas M. Miller, Raymond J. Bemish, and A. A. Viggiano*

Space Vehicles Directorate, Air Force Research Laboratory, Hanscom Air Force Base, Massachusetts 01731-3010, USA

(Received 31 August 2010; published 6 January 2011)

The mutual neutralization of anions with Ar^+ has been studied by variable electron and neutral density attachment mass spectrometry. Evidence of a previously unobserved plasma loss process, electron-catalyzed mutual neutralization (ECMN), e.g., $\text{SF}_6^- + \text{Ar}^+ + e^- \rightarrow \text{neutrals} + e^-$, is reported. Results for 10 species suggest that ECMN occurs generally and significantly affects the total ion-loss rate in plasmas with electron densities exceeding 10^{10} cm^{-3} . ECMN is discussed in the context of other known three-body plasma processes, the mechanisms for which appear insufficient to explain the observed effect. A mechanism for ECMN involving an incident electron facilitating energy transfer to the internal modes of the anion is proposed.

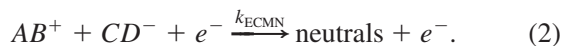
DOI: 10.1103/PhysRevLett.106.018302

PACS numbers: 82.20.-w, 82.33.Xj, 82.40.-g

Densities in weakly ionized plasmas are limited by the rate of charge loss processes: ion-electron recombination and ion-ion neutralization. These reactions proceed by two-body mechanisms with varying degrees of efficiency, and at high density the rates may be significantly enhanced via ternary mechanisms. Neutral third bodies enhance the rates at densities of 10^{17} – 10^{19} cm^{-3} (i.e., atmospheric pressures) [1–5]. When the slowest loss process, radiative recombination, dominates, the rate at which ions recombine with electrons is increased by collision with electron third bodies as well [6,7]. However, no evidence of high electron densities enhancing the rate of any other plasma loss process has previously been reported. In this Letter we present evidence that the rate of ion-ion mutual neutralization (MN)



is significantly increased by interaction with an electron, a process termed here electron-catalyzed mutual neutralization (ECMN),



Flowing afterglow (FA) apparatuses have been workhorses of plasma chemistry kinetics for five decades [8,9]. We have recently developed a new FA method, variable electron and neutral density attachment mass spectrometry (VENDAMS) [10], for measuring otherwise difficult to access kinetics including electron attachment to short-lived radicals and the neutral product distributions of MN. In extending the technique to higher plasma densities, we have found evidence of ECMN. At 300 K, ECMN becomes significant relative to MN at electron densities exceeding 10^{10} cm^{-3} , and may be the dominant mechanism for anion loss in high charge density plasmas containing a monatomic cation.

Both the FALP apparatus (Fig. 1) and VENDAMS technique have been described in detail elsewhere [10]. Briefly,

a microwave discharge produces a helium-electron plasma, which is carried down a 7 cm diameter stainless-steel-lined glass tube by a helium buffer gas. Argon, 2%–5% of the helium flow, is added to convert metastable helium and He_2^+ to Ar^+ , and the resulting plasma has >95% of positive charge as Ar^+ , with the remainder primarily He^+ . The neutral gas density is typically $3.2 \times 10^{16} \text{ cm}^{-3}$ (1 torr at 300 K). The electron density at the location of a glass neutral gas inlet ($[e^-]_{t=0}$) is varied by (a) moving microwave discharge, (b) changing the microwave power, and (c) moving some of the helium flow to the Ar port. The accessible range of $[e^-]_{t=0}$ is 1×10^8 to $5 \times 10^{10} \text{ cm}^{-3}$ as measured using a movable Langmuir probe. The ambipolar diffusion rate and plasma velocity are measured through procedures described elsewhere [10]. The relative concentrations of ionic species at the end of the flow tube are determined using a quadrupole mass spectrometer. Because the plasma velocity is known, the reaction time between the neutral inlet and the sampling aperture of the mass spectrometer is also known, typically 4.5 ms. Anions are formed via electron attachment to neutrals added at the fixed inlet after the Ar^+ /electron plasma has been established. The experiments here were performed at room temperature. Because of the density of the buffer gas, ions formed in the flow tube undergo thousands of collisions with neutral He and most species are assumed to be

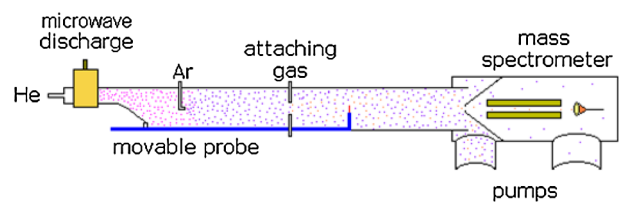


FIG. 1 (color online). A sketch of the FALP apparatus. Gas flow is from left to right. Locations of the helium, argon, and neutral attaching gas inlets are indicated.

thermalized; full details of the assumed interactions are presented elsewhere [11].

The rate constants for neutralization of Ar^+ with the anions are determined from kinetic modeling of experimental product anion branching ratios as a function of $[e^-]_{t=0}$. Modeling is described in detail elsewhere [10,12]. It is informative to note that the kinetics are calculated assuming all reactions energetically accessible between species known (ions) or inferred (corresponding neutrals) to be present are possible; however, only a small subset of the fastest reactions between the most abundant species have a measurable effect on the product anion abundances. The reactions considered for the SF_6 example discussed below are reported in detail elsewhere [11]. Calculated relative anion abundances are determined by iteratively solving the coupled differential equations describing the production and destruction of each species in the flow tube for the known reaction time and are compared to the experimental abundances via a weighted least squares goodness of fit. The calculations assume that the rate constants of all reactions may vary across plausible ranges determined from prior experiments or collisional limits. The best-fit and uncertainty limits quoted below represent a full sampling of the large parameter space through a Monte Carlo optimization procedure.

The absolute neutralization rate constant of an anion (illustrated here for SF_6^-) with Ar^+ is determined by monitoring the anion abundance relative to that of an atomic anion that, because it neutralizes at a negligible rate [13], acts as an internal standard. Because electron attachment to SF_6 does not produce an atomic ion, a second gas, CCl_4 , is added to produce Cl^- . Figure 2 shows the fractions of SF_6^- and Cl^- as a function of $[e^-]_{t=0}$ for two different initial concentrations of CCl_4 : one high enough to reduce the electron density to zero at short times [Fig. 2(a)], and the other low enough that electrons persist throughout the entire reaction time [Fig. 2(b)]. To emphasize the difference in the $[e^-]$, a line representing $\langle [e^-] \rangle$ is shown in each panel. The modeling of case A is straightforward: only electron attachment to SF_6 and CCl_4 and one mutual neutralization process contribute significantly, although other reactions are included in the modeling. Importantly, because the large concentration of CCl_4 depletes the electron density rapidly, $\langle [e^-] \rangle$ is low and ECMN is suppressed. The attachment reactions are well studied [14], leaving only the MN rate constant (k_{MN}) as a variable. At $t = 0$, the Ar^+ concentration is equal to $[e^-]_{t=0}$; at low $[e^-]_{t=0}$ little MN occurs, and as $[e^-]_{t=0}$ increases, MN causes the SF_6^- abundance to decrease, while Cl^- , which does not react with Ar^+ , remains unaffected. This leads to the curvature seen in Fig. 2(a). The thick and thin lines in Fig. 2(a) represent the best-fit value of k_{MN} and experimental error limits, respectively. Importantly, the determination does not rely on a measurement of the absolute ion density using the Langmuir probe, which has been shown

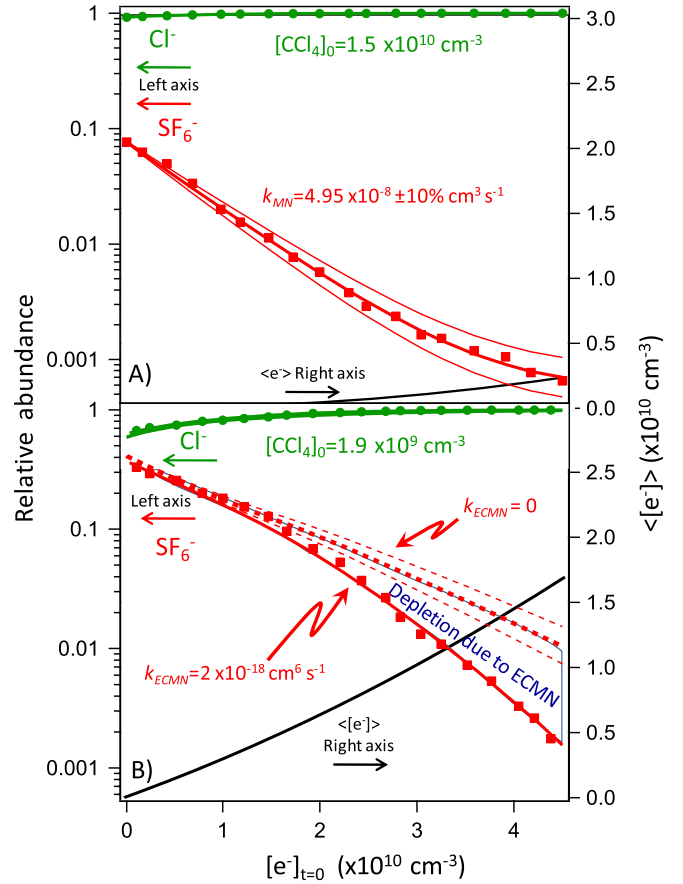
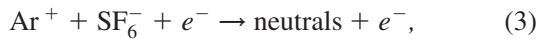


FIG. 2 (color online). Relative product anion abundances [$e.g.$, $[\text{SF}_6^-]/([\text{SF}_6^-] + [\text{Cl}^-])$] after 4.5 ms reaction time on addition of $1.9 \times 10^9 \text{ cm}^{-3}$ SF_6 and the indicated amounts of CCl_4 to the flowing afterglow as a function of electron density at the neutral injector ($[e^-]_{t=0}$). Thick solid lines are best-fit modeled abundances. Dashed lines in (b) are the best-fit modeled abundances assuming the range of k_{MN} determined in (a) and excluding ECMN; the solid lines in (b) are the best-fit modeled abundances including ECMN. The primary difference between (a) and (b) is the amount of electron depletion due to attachment to CCl_4 ; the degree of this difference is indicated by the modeled average electron density throughout the full reaction time ($\langle [e^-] \rangle$) as a function of $[e^-]_{t=0}$ (solid lines, right axis) under each condition.

to be inaccurate [15]. Case B involves additional processes due to electron reactions, all of which are understood and detailed elsewhere [11] (these are included but negligible in case A). Here we focus only on the total neutralization rate although all rate parameters are varied in the modeling. Assuming the k_{MN} determined in case A and no ECMN, the data are fit poorly, as evidenced by the dashed line in Fig. 2(b). In case B, $\langle [e^-] \rangle$ increases dramatically at high $[e^-]_{t=0}$. The deviation between model and experiment is proportional to $[e^-]_{t=0}$. In order to explain the data, an additional loss process, which has the rate dependence of MN with an extra proportionality to $[e^-]$, needs to be included. We have explored a number of potential reactions but only ECMN,



yields an excellent fit; see the solid line in Fig. 2(b). The difference between the solid and dashed lines shows the increasing importance of ECMN with increasing $\langle [e^-] \rangle$. The reported three-body rate constant of $2 \times 10^{-18} \binom{+2}{-1} \text{cm}^6 \text{s}^{-1}$ (where the numbers in the parentheses represent asymmetric uncertainty limits) is in fact relative to the undetermined ECMN rate constant of Cl^- and Ar^+ , which is assumed to be negligibly small. This result is not confined to SF_6^- ; we have measured nonzero ECMN rate constants for several other systems, as discussed below.

We now address the possible mechanism of ECMN and its relationship to previously described mechanisms of MN and of the enhancement of MN by a neutral third body. The theory of MN of atomic ions was detailed by Flannery [2]. The basic concept is that anions have a hydrogenlike orbital that extends far from the atomic center; when there is a sufficient overlap between the ions and constraints on the energy, momentum, spin, and symmetry are met, the electron transfers. In terms of gas phase rates, the MN process has to be averaged over a range of impact parameters which generate orbital angular momentum. The picture may be extended to polyatomic species, where the additional vibrational degrees of freedom make it much more likely that energy, momentum, spin, and symmetry constraints are met, causing the MN rate constants for polyatomic species to be orders of magnitude higher than MN of two atomic species, a feature exploited in the present measurements. Because MN relies on the hydrogenic orbital overlap, k_{MN} can be directly correlated to the square root of the electron binding energy (EBE) of the anion [16]. The relative ion velocity affects the crossing between ionic and neutral product potential surface; therefore, k_{MN} also depends on the reduced mass of the complex. For polyatomic anions [11], there is a critical interior radius (R_c) that, if crossed, commits the ion pair to MN. Because ECMN is additive to MN, the events that lead the ion pair to ECMN must occur outside of R_c . To date we have studied ECMN in ten species, and interestingly, unlike k_{MN} [17], no correlation to the reduced mass or the EBE was found, suggesting that it is a fundamentally different process.

In the analogous neutral third-body enhanced MN, a neutral species collides with the ion-ion complex and removes some of the kinetic energy [1,18]. This traps the complex in the attractive well and allows what would otherwise be a low probability neutralization to occur. In ECMN, the electron third body is a poor collisional energy sink due to the extreme mass difference. For ECMN to be as efficient as observed, it must proceed by a different mechanism and transfer energy from the ion-ion complex to a degree of freedom other than the kinetic energy of the electron. The only readily available energy sinks in the current systems are the internal modes of the polyatomic anion. If an electron allows some of the kinetic energy of

the ion-ion complex to be transferred to the vibrational modes of the anion, it would trap a complex that would otherwise not have crossed R_c . From the perspective of the anion, the ionic potential created by the attraction of a cation disappears and reappears as an electron passes between the pair, creating an electromagnetic fluctuation. At 300 K, the center frequency for this fluctuation is on the order of thermal energy ($\sim 200 \text{ cm}^{-1}$), in the same range as low frequency vibrational modes. Additionally, the ion-ion pair attraction distorts the anion geometry, which would be expected to be temporarily restored to the zero-field value as the electron eclipses the cation charge. The result of the change of internal geometry of the anion is a time dependent change in the dipole, in other words, a transition dipole. Because the transit time of the thermal electron, and therefore the frequency of the fluctuation, is similar to the time scale of the vibration, the geometry change induced by the addition and removal of a distortion in the potential may leave the mode in a more excited state than before the interaction. Effectively, a photon may be absorbed, removing kinetic energy from the center of mass frame of the cation-anion system. Figure 3 shows this schematically for the simple case of an electron passing perpendicularly to the ion-pair axis in the same plane. The physics of this mechanism are not novel, as a similar effect has been previously observed in the case of diffuse electrons exciting neutral vibrations when ejected from dipole-bound anions [19].

An evaluation of the mechanism through comparison of the measured magnitude of ECMN to rigorous theory, e.g. R -matrix calculations [20], is possible, but difficult,

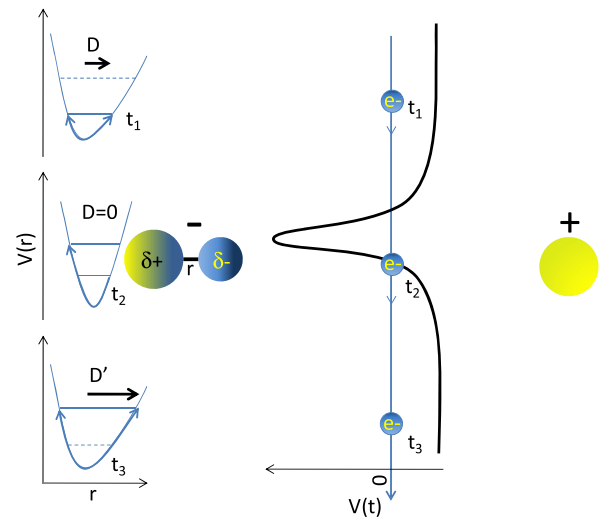


FIG. 3 (color online). Schematic representation of the proposed ECMN mechanism. An electron passing between the charged species (shown at three discrete time steps) shields the positive charge, inducing an electromagnetic fluctuation $[V(t)]$. The corresponding distortion in the potential seen by the anion $[V(r)]$ results in a changing dipole (D), allowing for coupling between the kinetic energy of the system and low energy vibrations of the anion.

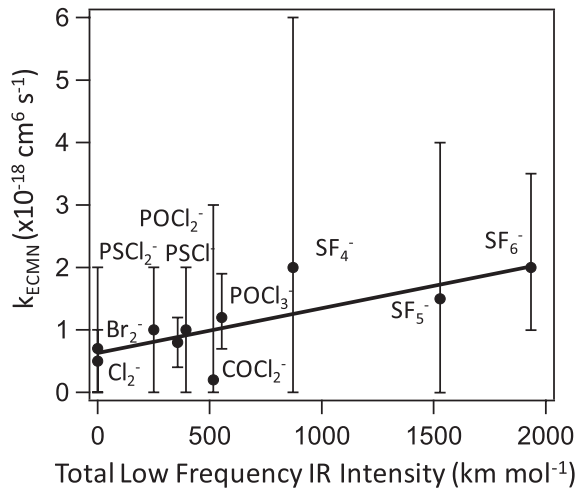


FIG. 4. Comparison of experimental ECMN rate constants for various anions with Ar⁺ at 300 K with calculated low energy IR intensity. Fit is a linear regression to the experimental points.

and is not attempted here. We do note that the magnitude of the enhancement should scale with the likelihood of low energy modes of the anion to absorb a photon. Figure 4 shows the correlation of summed sub-800 cm⁻¹ IR intensity [GAUSSIAN quantum chemical software [21]; B3LYP/6-311+G(d)] to the measured ECMN rate constant. The 800 cm⁻¹ cutoff is arbitrary and intended to include only energies likely to be excited by room temperature electrons, but the results are robust for cutoffs several hundred cm⁻¹ higher or lower. The correlation (R^2) is 0.5, which is significantly higher than the values for correlation to anion mass, EBE, exothermicity of the neutralization, and dipole of the anion, all having R^2 values below 0.07. For comparison, the well-established relationship between k_{MN} and EBE has an R^2 value of only 0.38. Interesting consequences for such a mechanism are that, for homonuclear diatomics such as Cl₂⁻, there should be no ECMN effect, and indeed, the rate constant is small. The intercept is nonzero, counter to what is expected from the proposed mechanism. It is of interest to identify any alternate mechanisms that could contribute to the observed ion-loss process.

This Letter highlights the discovery of a new loss process for moderately high electron density plasmas. Prior to this Letter, electrons had been documented as an effective third body for only one plasma loss process: radiative recombination [6,7], via a mechanism for enhancement through elastic collision, with experimental rate constants well reproduced by a simple extension of Thomson's classical description of neutral third-body enhancement of MN [22]. The present results show that moderate electron densities also increase the total neutralization rate constant. A typical ECMN rate constant is 10–100 times larger than that of collisional-radiative recombination, 10⁶ times larger than that of any process with a neutral third body, and the collisional mechanism is insufficient to explain the magnitude of the effect. Instead, a mechanism involving

the coupling of vibrational modes of the anion to the kinetic energy of the system is proposed. ECMN has been measured only up to electron densities of 5×10^{10} cm⁻³, but, like neutral third-body rates, the effect must reach a maximum at some higher density. This leaves just one loss process that has not yet been shown to be enhanced by interaction with electrons: dissociative recombination. Because of the fast two-body rate of dissociative recombination, collisional electron enhancement likely becomes significant only at electron densities above 10^{11} cm⁻³, out of reach of our current instrumentation. It is plausible that electron-catalyzed dissociative recombination will occur by this or an alternate mechanism, the important question being whether the rate enhancement is significant under realistic plasma conditions.

We are grateful for the support of the Air Force Office of Scientific Research for this work. T.M.M. is under contract to the Institute for Scientific Research of Boston College. N.S.S. is supported by the National Research Council Research Associateship Program.

*Corresponding author.

- [1] D.R. Bates and I. Mendaas, *Chem. Phys. Lett.* **88**, 528 (1982).
- [2] M.R. Flannery, *Phil. Trans. R. Soc. A* **304**, 447 (1982).
- [3] M. Larsson and A.E. Orel, *Dissociative Recombination of Molecular Ions* (Cambridge University Press, Cambridge, England, 2008).
- [4] J. Glosik *et al.*, *Phys. Rev. A* **80**, 042706 (2009).
- [5] G.A. Fisk, B.H. Mahan, and E.K. Parks, *J. Chem. Phys.* **47**, 2649 (1967).
- [6] E. Hinnov and J.G. Hirschberg, *Phys. Rev.* **125**, 795 (1962).
- [7] D.R. Bates and A.E. Kingston, *Nature (London)* **189**, 652 (1961).
- [8] E.E. Ferguson, F.C. Fehsenfeld, and A.L. Schmeltekopf, in *Advances in Atomic and Molecular Physics*, edited by D.R. Bates (Academic, New York, 1969), p. 1.
- [9] S.T. Graul and R.R. Squires, *Mass Spectrom. Rev.* **7**, 263 (1988).
- [10] N.S. Shuman, T.M. Miller, C.M. Caples, and A.A. Viggiano, *J. Phys. Chem. A* **114**, 11 100 (2010).
- [11] J.C. Bopp *et al.*, *J. Chem. Phys.* **129**, 074308 (2008).
- [12] N.S. Shuman *et al.*, *J. Chem. Phys.* (to be published).
- [13] M.J. Church and D. Smith, *J. Phys. D* **11**, 2199 (1978).
- [14] D. Smith, N.G. Adams, and E. Alge, *J. Phys. B* **17**, 461 (1984).
- [15] R. Johnsen, E.V. Shunko, T. Gougousi, and M.F. Golde, *Phys. Rev. E* **50**, 3994 (1994).
- [16] A.P. Hickman, *J. Chem. Phys.* **70**, 4872 (1979).
- [17] T.M. Miller, *J. Chem. Phys.* **72**, 4659 (1980).
- [18] J.J. Thomson, *Philos. Mag. Ser. 6* **47**, 337 (1924).
- [19] C.G. Bailey, C.E.H. Dessent, and M.A. Johnson, *J. Chem. Phys.* **104**, 6976 (1996).
- [20] J. Tennyson, *Phys. Rep.* **491**, 29 (2010).
- [21] GAUSSIAN, M.J. Frisch *et al.* (Gaussian, Inc., Pittsburgh PA, 2003).
- [22] N. D'Angelo, *Phys. Rev.* **140**, A1488 (1965).